

This article was downloaded by:

On: 26 January 2011

Access details: *Access Details: Free Access*

Publisher *Taylor & Francis*

Informa Ltd Registered in England and Wales Registered Number: 1072954 Registered office: Mortimer House, 37-41 Mortimer Street, London W1T 3JH, UK



## Liquid Crystals

Publication details, including instructions for authors and subscription information:

<http://www.informaworld.com/smpp/title~content=t713926090>

### Novel liquid crystalline structures of a chiral side chain polymer and its phase transitions

L. S. Li<sup>a</sup>; X. J. Hong<sup>a</sup>; S. I. Stupp<sup>ab</sup>

<sup>a</sup> Departments of Materials Science and Engineering, Beckman Institute for Advanced Science and Technology, University of Illinois, Urbana, IL, U.S.A <sup>b</sup> Departments of Chemistry Materials Research Laboratory, Beckman Institute for Advanced Science and Technology, University of Illinois, Urbana, IL, U.S.A

**To cite this Article** Li, L. S. , Hong, X. J. and Stupp, S. I.(1996) 'Novel liquid crystalline structures of a chiral side chain polymer and its phase transitions', *Liquid Crystals*, 21: 4, 469 – 483

**To link to this Article:** DOI: 10.1080/02678299608032856

**URL:** <http://dx.doi.org/10.1080/02678299608032856>

PLEASE SCROLL DOWN FOR ARTICLE

Full terms and conditions of use: <http://www.informaworld.com/terms-and-conditions-of-access.pdf>

This article may be used for research, teaching and private study purposes. Any substantial or systematic reproduction, re-distribution, re-selling, loan or sub-licensing, systematic supply or distribution in any form to anyone is expressly forbidden.

The publisher does not give any warranty express or implied or make any representation that the contents will be complete or accurate or up to date. The accuracy of any instructions, formulae and drug doses should be independently verified with primary sources. The publisher shall not be liable for any loss, actions, claims, proceedings, demand or costs or damages whatsoever or howsoever caused arising directly or indirectly in connection with or arising out of the use of this material.

# Novel liquid crystalline structures of a chiral side chain polymer and its phase transitions

by L. S. LI†, X. J. HONG†, and S. I. STUPP\*†‡

Departments of Materials Science and Engineering† and Chemistry‡ Materials Research Laboratory, Beckman Institute for Advanced Science and Technology, University of Illinois at Urbana-Champaign Urbana, IL 61801, U.S.A.

(Received 15 October 1995; in final form 23 April 1996; accepted 24 April 1996)

Two novel smectic bilayer structures have been identified in an enantiomerically enriched chiral side chain polymer containing the highly dipolar nitrile group at stereocentres. The structures were characterized by electron diffraction, electron microscopy, and X-ray diffraction. In both phases each smectic layer has a bilayer structure with backbones and spacers confined in a thin disordered region between two sublayers of mesogenic segments. One of the structures which we denote as CrE\* has the unusual feature of having its side chains arranged parallel to the layer normal in spite of its enantiomeric bias and twisted nature. In the second structure side chains are tilted by  $34.8^\circ$  with respect to the layer normal and we denote this phase as CrH\*. In both structures each sublayer contains three different orientations of orthorhombic (CrE\*) or monoclinic (CrH<sub>c</sub>\*) lattices which are related to one another by rotations of  $\pm 60^\circ$  about the *c*-axis. In both the CrH<sub>c</sub>\* and the CrE\* phases, lattices in each sublayer are regularly rotated about the *c*-axis by  $5.9^\circ$  relative to those in the adjacent sublayer. The observation of a chiral CrH phase is uncommon and in this specific case the structure is unique since the rotation between adjacent layers occurs about the side-chain axis (*c*-axis) (CrH<sub>c</sub>\*) and not about the layer normal (*c*\*-axis) (CrH\*). We believe the system undergoes a change in molecular organization from CrH<sub>c</sub>\* to CrE\* as a result of a chemical reaction which joins a fraction of the stereocentres through covalent bonds. With increasing temperature the CrE\* structure was found to transform to a special orthorhombic untwisted smectic phase in which  $a = 3^{1/2}b$ , denoted here as CrE<sub>h</sub>. The structure then transforms to a hexatic S<sub>B</sub> phase and finally to a S<sub>A</sub> phase at yet higher temperatures.

## 1. Introduction

A few years ago our laboratory synthesized the enantiomerically enriched oligomer **S-1** containing at its stereocentre the highly dipolar nitrile group, having a dipole moment of approximately 3.4 Debye units. This compound has an enantiomeric excess value of approximately 0.75 or higher and was found to exhibit liquid crystalline phases. A very similar but not identical *R* enantiomer (**R-1**) had also been synthesized earlier in our laboratory and at temperatures close to and above its isotropization temperature of  $98^\circ\text{C}$ , the acrylate and nitrile groups of this compound were found to react 'in bulk' to form two-dimensional (2D) polymers through the formation of short polyacrylate and polyimine backbones [1, 2]. We also synthesized the side chain polymer **S-2** through dilute solution free radical polymerization of **S-1**.

In this work we have studied the structure of the 'side chain' polymer **S-2** in an effort to understand the effect that a strong dipole moment at the stereocentre might

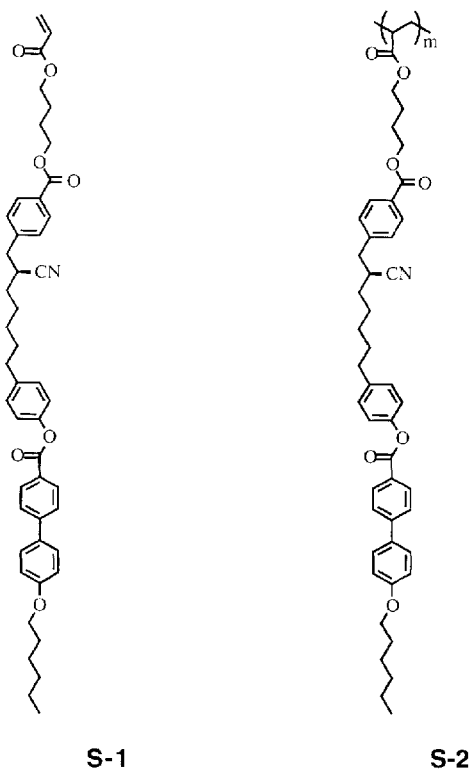
have on the system's molecular organization. We had recently reported on the important structural role played by this type of stereocentre in polymers of 'main chain' architecture [3]. One of our objectives here has been to understand the role of architecture on molecular organization by comparing structurally the one-dimensional covalent structure **S-2** to the analogous two-dimensional structure obtained previously by bulk polymerization of **R-1**. The structural characterization of **S-2** was carried out by electron microscopy, electron diffraction and X-ray diffraction. Hot stage electron diffraction was also used in order to study the material's phase transitions.

## 2. Experimental

### 2.1. Synthesis

The synthesis of **S-1** was carried out using a procedure similar but not identical to that described before for the *R* enantiomer [2]. The *S* enantiomer was synthesized using the chiral auxiliary (*S*)-1-amino-2-(methoxymethyl)pyrrolidine and the methodology used to obtain nitrile groups has been previously described by our group [4]. In fact, the 21-step synthesis of **S-1** differed

\* Author for correspondence.



from that previously described for the *R* enantiomer in the methodology used to convert chiral hydrazones to nitriles. The synthesis of **S-1** utilized the amidine base 1,5-diazabicyclo[4.3.0]non-5-ene to eliminate a diastereomerically enriched hydrazone iodide to a nitrile at

$-78^{\circ}\text{C}$ . This methodology was developed in our laboratory and was reported in detail previously [5]. The enantiomeric excess of **S-1** was measured by NMR using chiral shift reagents following a method described in one of our previous publications [4]. As mentioned above **S-1** has an enantiomeric excess value of at least 0.75.

### 2.2. Sample preparation

Thin films of the polymer were prepared using a 0.1 % by weight solution in chloroform. A few drops of this solution were placed on the surface of glycerin preheated to  $110^{\circ}\text{C}$  or  $77^{\circ}\text{C}$ . Solutions spread easily on the glycerin surface and solvent evaporation occurred rapidly, generating thin films of the sample. Films were then slowly cooled to room temperature at a rate of approximately  $3^{\circ}\text{C min}^{-1}$ . After films were rinsed several times in deionized water in order to remove residual glycerin, they were picked up on 3 mm diameter copper grids for electron diffraction and electron microscopy examination. The thicker portions of similar films were picked up on microscope slides for X-ray diffraction analysis.

### 2.3. Electron microscopy, electron diffraction and X-ray diffraction

Thin films of the polymer were examined using two different electron microscopes, a Philips CM-12 and a Philips EM420, both operated at 120 KV. The camera length was calibrated using  $\text{TiCl}_3$  evaporated onto the thin films. Heating experiments to characterize phase transitions of the films utilized the Philips EM420 which is equipped with a hot stage, and all thin films for

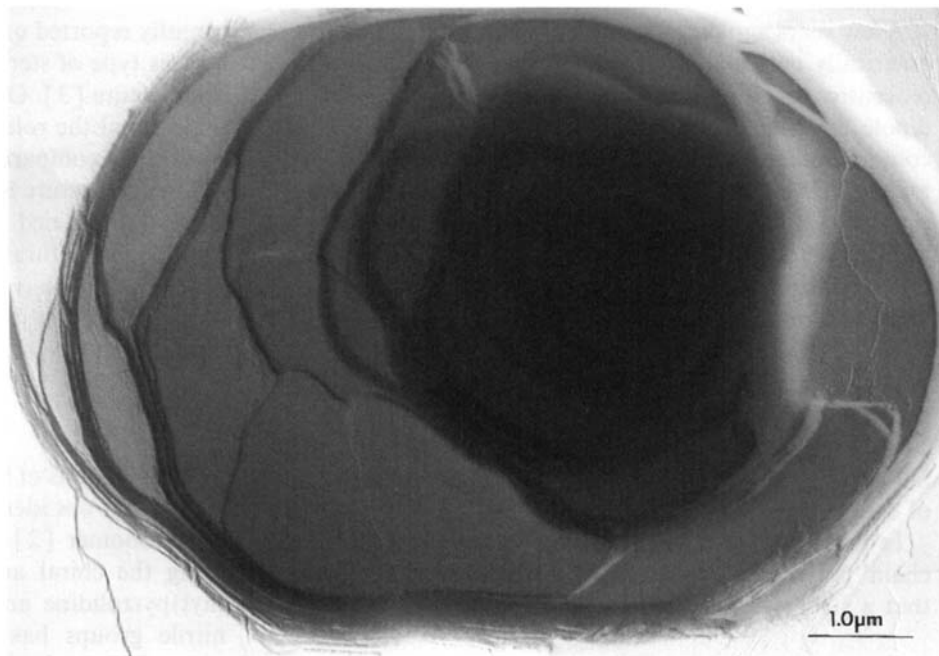


Figure 1. Transmission electron micrograph of a film of the side chain polymer in the CrE\* phase. The film was cast from solution at  $110^{\circ}\text{C}$ .

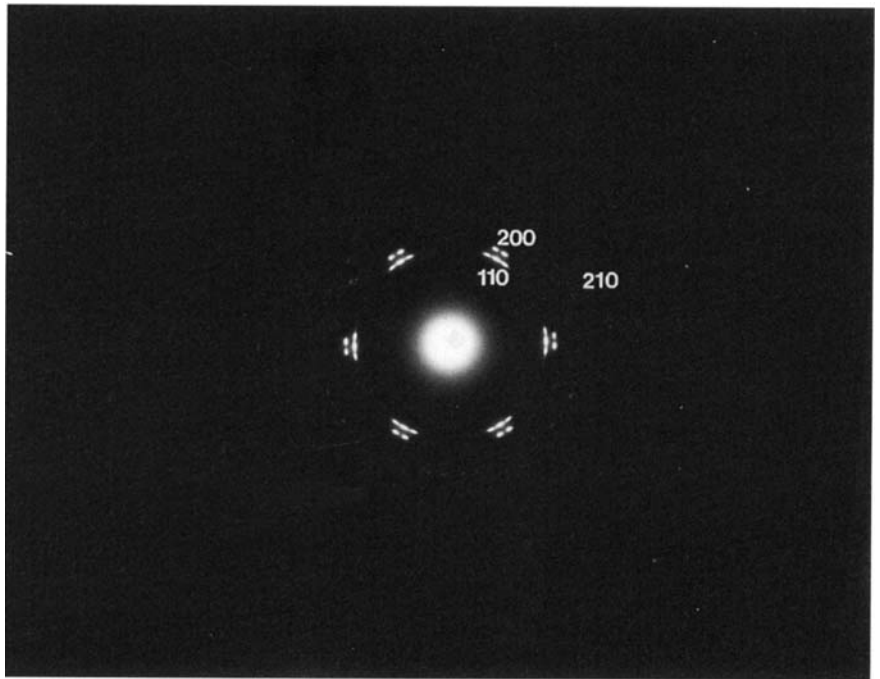


Figure 2. Selected area electron diffraction pattern of a thin film in the CrE\* phase.

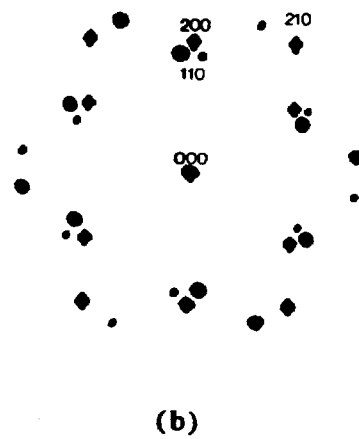
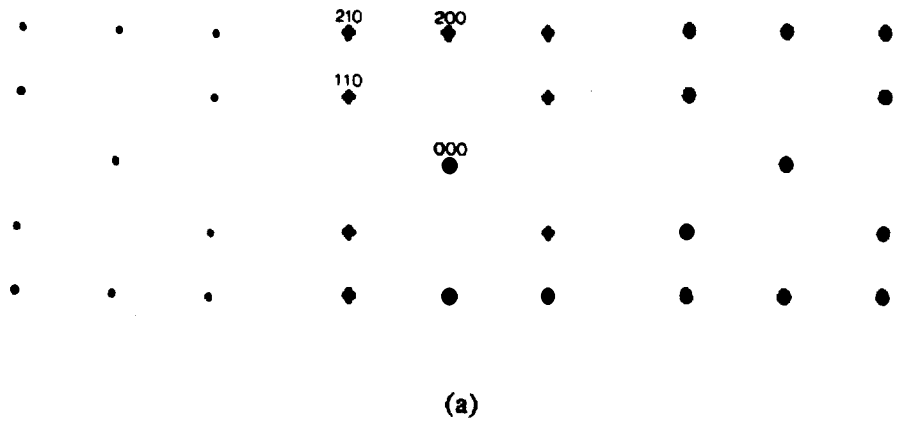


Figure 3. (a) Schematic representation of three orthorhombic  $a^*b^*$  reciprocal lattice planes. (b) Relative rotations of  $\pm 60^\circ$  of the three  $a^*b^*$  reciprocal lattice planes about the  $c$  axis generate a diffraction pattern with hexagonal geometry.

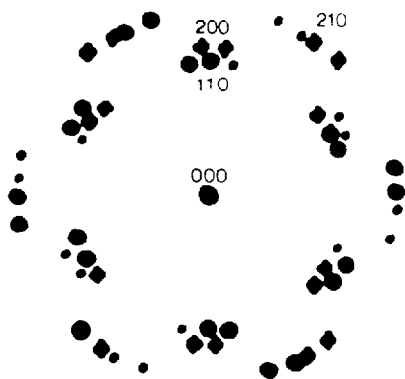


Figure 4. Schematic representation of  $a^*b^*$  reciprocal lattice planes corresponding to two sublayers rotated by  $5.9^\circ$  relative to each other about the  $c$  axis.

electron microscopy were first shadowed with Pt-C in order to enhance image contrast. X-ray diffractograms were obtained using a Rigaku/D-Max diffractometer in the reflection mode with  $\text{CuK}\alpha$  radiation.

### 3. Results and discussion

#### 3.1. The chiral crystal $E$ phase ( $\text{CrE}^*$ ) of the polymer

Figure 1 is an electron micrograph of a film of **S-2** obtained by solution casting on a glycerin surface preheated to  $110^\circ\text{C}$ . This figure shows clearly that films consist of layers stacked parallel to each other. Figure 2

is a selected area electron diffraction pattern of a thin region of the film (approximately  $50\text{ \AA}$  thick) which reveals reflection spots distributed with hexagonal geometry. However, this pattern cannot be indexed by hexagonal unit cell parameters, requiring instead the following orthorhombic parameters;  $a=8.24\text{ \AA}$ ,  $b=5.34\text{ \AA}$  and  $\gamma=90^\circ$ .

Since this pattern contains only  $hk0$  reflections, we conclude that the  $c$  axis (side-chain axis) is parallel to the layer normal and therefore perpendicular to the film plane. The observed  $d$ -spacings and their indices have been listed in table 1. The hexagonal geometry of the distribution of  $hk0$  reflections in the pattern can be explained by three different orientations of orthorhombic reciprocal lattices related to one another by  $\pm 60^\circ$  rotations about the  $c$  axis. This is shown schematically in figure 3 for a single layer. The hypothetical pattern shown in figure 3(b) contains two 110, one 200 and two 210 reciprocal lattice points. However, the actual pattern shown in figure 2 reveals three 110 reflections, two 200 reflections and four 210 reflections. If the reciprocal lattices of two neighbouring layers are rotated by  $5.9^\circ$  about the  $c$  axis relative to each other one observes exactly the pattern shown in figure 2. We therefore interpret the pattern as resulting from a bilayer structure in which the two sublayers are twisted by a small angle relative to each other. Figure 4 shows the superposition of orthorhombic  $a^*b^*$  reciprocal lattice planes in two

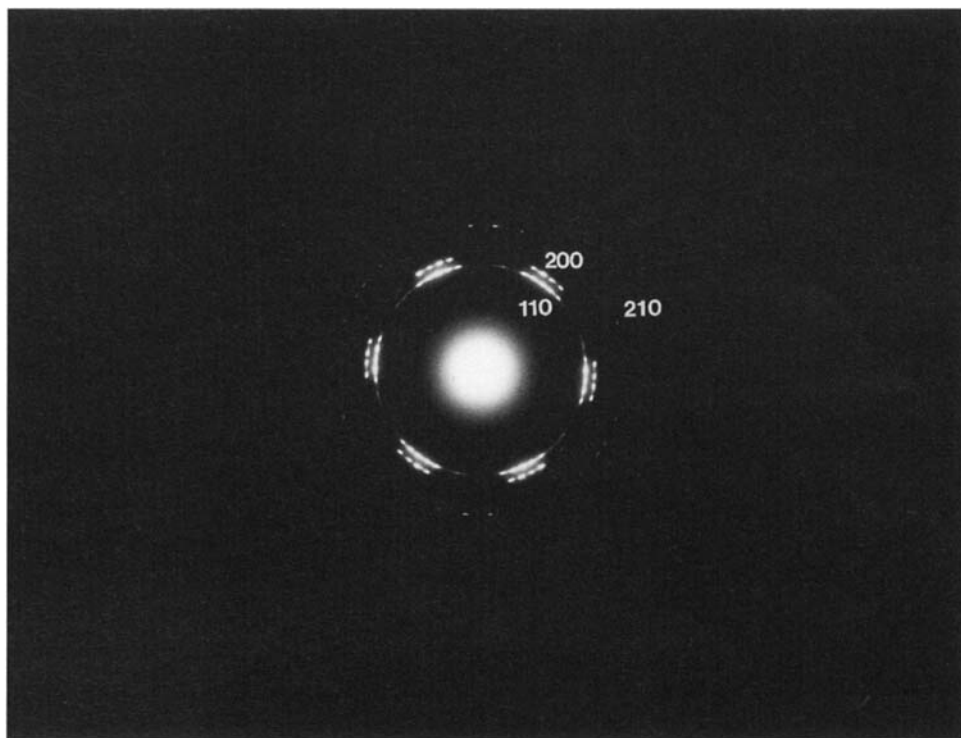


Figure 5. Selected area electron diffraction pattern of two bilayers of the side-chain polymer in the  $\text{CrE}^*$  phase.

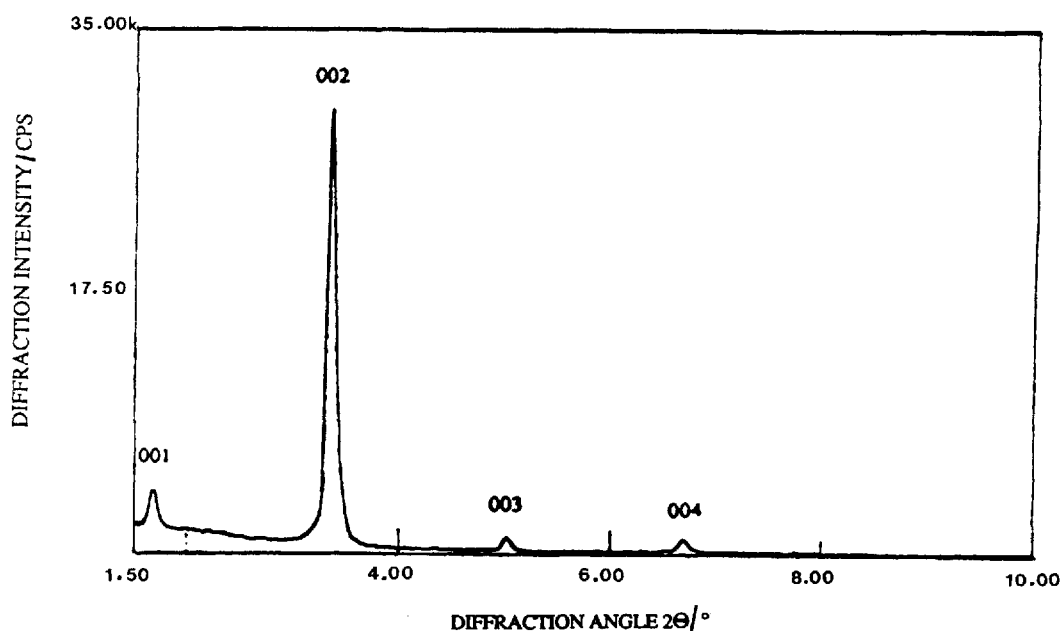


Figure 6. X-ray diffraction scan of the polymeric film in the CrE\* phase.

sublayers rotated by  $5.9^\circ$  relative to each other. Each sublayer consists of three different orientations of the orthorhombic  $a^*b^*$  reciprocal lattice planes which are related to one another by rotations of  $\pm 60^\circ$ . Also, in this simulated pattern the angle between every two neighbouring  $[110]^*$  and between every two neighbouring  $[200]^*$  reciprocal vectors is  $5.9^\circ$ . It is clear that the simulated pattern in figure 4 matches fairly well the experimental pattern shown in figure 2. Figure 5 is another selected area electron diffraction pattern of a thin film of the polymer, showing five 110 and four 200 reflections. Again, the angle between every two neighbouring  $[110]^*$  or every two neighbouring  $[200]^*$  is  $5.9^\circ$ . Therefore, this pattern can be interpreted as one resulting from 4 sublayers and the  $5.9^\circ$  twist between sublayers is characteristic of this molecular structure.

Based on electron diffraction as well as X-ray diffraction results described below, one may conclude with certainty that this side chain polymer is organized as a bilayer structure. The number of 110 reflections in the electron diffraction patterns is always odd and larger than or equal to 3. On the other hand, the number of 200 spots is always even and larger than or equal to 2. This implies, of course, the presence of a bilayer structure. Furthermore, figure 6 shows an X-ray diffraction scan of a film sample, revealing 4 sharp reflections (001, 002, 003, 004). The  $2\theta$  position of these peaks indicates that bilayers in this side chain polymer are  $52.6 \text{ \AA}$  thick. This thickness is larger than the length of one fully extended side-chain ( $\sim 46 \text{ \AA}$ ) and shorter of course than two of them. It is therefore reasonable to suggest that a bilayer

structure exists in this polymer. The difference in thickness between that of a bilayer of fully extended side chains ( $\sim 92 \text{ \AA}$ ) and the observed thickness of  $52.6 \text{ \AA}$  can be accounted for by at least two factors. One would be a non-extended conformation of side chains (including spacers), and another factor would be the interdigitation of side chains in the structure. It is very important to note that the second order reflection in the X-ray scan is much stronger than the first one. Based on the work of Davidson and Levelut [6], this implies that the electron density profile along the  $c$  axis within the layer is not a single sinusoidal function. A plausible explanation is therefore that the central region of the bilayer occupied by backbones and spacers is of lower density and more disordered than the rest of the bilayer. A schematic representation of the bilayer is shown in figure 7.

In summary, the samples obtained from solutions cast on glycerin at  $110^\circ\text{C}$  exhibit a crystal E-like structure at room temperature. If there were no twisting between layers in the film the structure would be typical of that found in crystal E phases. However, in this case a  $5.9^\circ$  twist angle between adjacent layers has been identified. This implies that a novel *orthogonal* smectic phase has been observed which one may refer to as a chiral crystal E phase (CrE\*). As far as we know molecules in most chiral smectic phases are tilted with respect to the layer normal, and we are not aware of previous reports on structures of chiral crystal E phases. There is, however, a vast literature on twisted smectic A\* phases formed by enantiomerically enriched chiral molecules (twist grain boundary phases) [7–12].

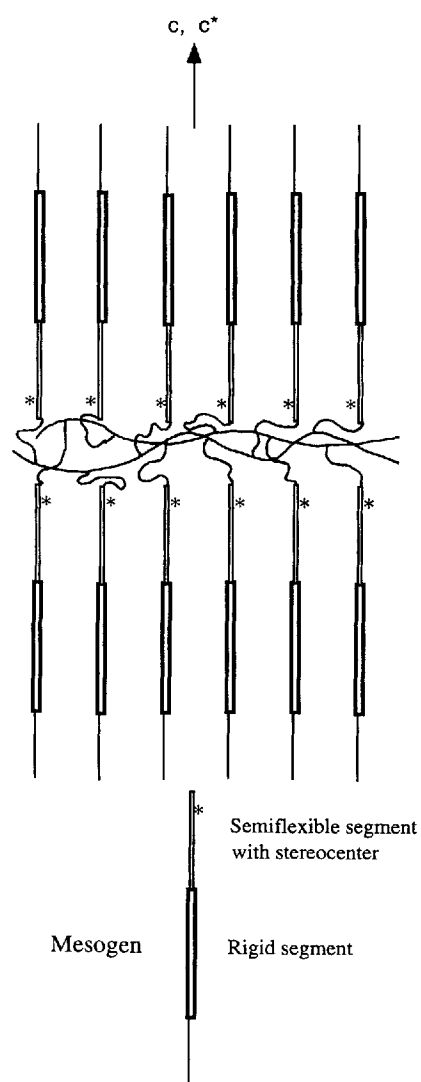


Figure 7. Schematic representation of a bilayer of the CrE\* phase, showing side-chains packed in parallel with polymer backbones and spacers confined in a thin disordered region between two mesogenic sublayers.

### 3.2. The chiral crystal $H_c$ phase $CrH_c^*$ of the polymer

When films of the polymer were cast on glycerin at 77°C as opposed to 110°C a very different morphology from that of the CrE\* phase was observed. Many 'dome-like' regions were found in the films, and figure 8 shows an example of these structures. Most importantly, the 'dome' is composed of layers that appear to be tilted with respect to the film's normal. Figure 9 is another electron micrograph taken from the thinnest part of the 'dome', showing the tilted layers in different domains. There are also visible defects observed in the micrograph, such as curved layers and edge dislocations. If a film is prepared at the intermediate temperature of 95°C, one obtains a mixed microstructure with morphologies char-

acteristic of the CrE\* phase (see figure 1) and those observed in films prepared at the lower temperature of 77°C (see figure 10). Figure 11 is a selected area electron diffraction pattern taken from one of the domains shown in figure 9. This pattern is similar to that of the chiral crystal E phase. The 110 and 200 reflection spots are separated and both of them are distributed with hexagonal geometry. This indicates that there are also orthogonal  $a^*b^*$  reciprocal lattice planes with their  $c$  axis (side-chain axis) parallel to the beam direction. Based on this observation we conclude that side-chain axes within the layers are not parallel to the layer normal. Because the reflection spots are distributed with hexagonal geometry there must be three different orientations of the orthogonal  $a^*b^*$  reciprocal lattice planes, related to each other by rotations of  $\pm 60^\circ$  about the  $c$  axis. There are many 110 and 200 reflection spots, and the angle between every two neighbouring  $[110]^*$  reciprocal vectors or every two neighbouring  $[200]^*$  reciprocal vectors is  $5.9^\circ$ . Therefore each tilted layer is also a bilayer and within each sublayer there are three different orientations of the orthogonal  $ab$  lattice planes (related to each other by rotations of  $\pm 60^\circ$  about the  $c$  axis). Furthermore, the lattices in each sublayer are then regularly rotated by  $5.9^\circ$  about the  $c$  axis relative to those in the adjacent sublayer. The observed rotation about the  $c$  axis is not, as far as we know, common in a chiral smectic phase. In fact, a homologous compound to S-1 (opposite configuration and a 5 carbon alkoxy tail) was found to have an CrH\* phase at room temperature but its twist occurs about the normal to the layers [2]. This homologous compound was used as a precursor in the synthesis of 2D polymers and this work is described elsewhere [1, 2]. Because of this difference it might be appropriate to describe one phase as CrH\* (the one with twisting about the layer normal,  $c^*$  axis), and the other phase (that of the S-2 described here) as CrH $_c^*$  in order to imply rotation about the side-chain axis ( $c$  axis). The  $d$ -spacings and indices for the electron diffraction pattern of S-2 shown in figure 11 are listed in table 2.

Figure 12 is a selected area electron diffraction pattern obtained from a tilted sample. This pattern shows not only 110 and 200 reflections, but also six small angle reflections, indicating that the thickness of the tilted layers is about 51 Å. This is consistent with the X-ray diffraction scan of the film shown in figure 13 revealing four 00l Bragg reflections from the tilted layers, corresponding to a period of 51.4 Å. Here again, the second order reflection is the strongest, indicating, as explained before, that a non-uniform density exists within the bilayer. Figure 14 shows the same X-ray diffraction results with a magnified intensity scale. In addition to the four sharp peaks, other broader peaks are observed

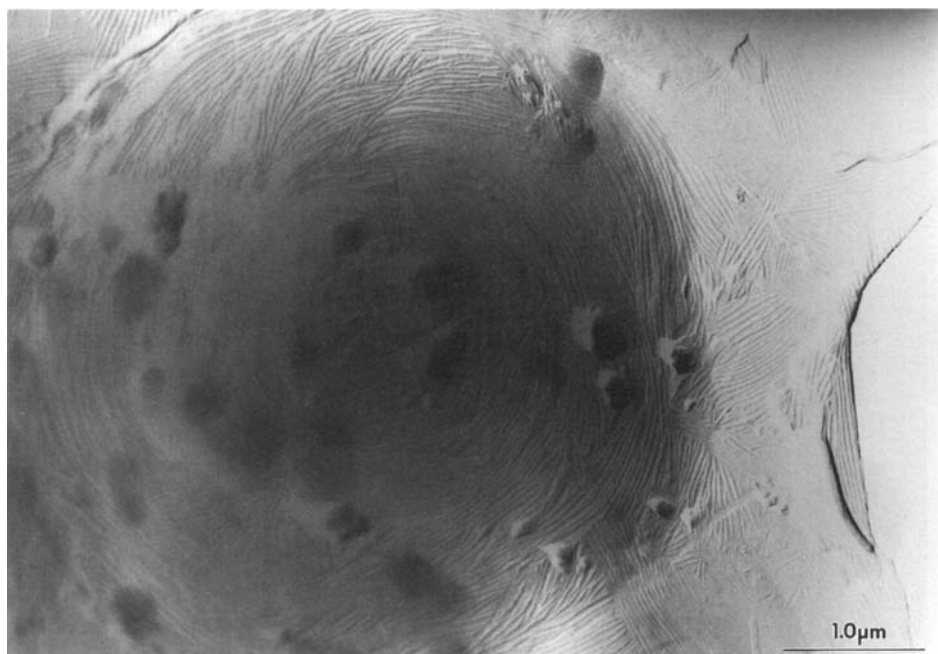


Figure 8. Transmission electron micrograph of a thin film of the side chain polymer in the  $\text{CrH}_c^*$  phase cast from solution at  $77^\circ\text{C}$ .

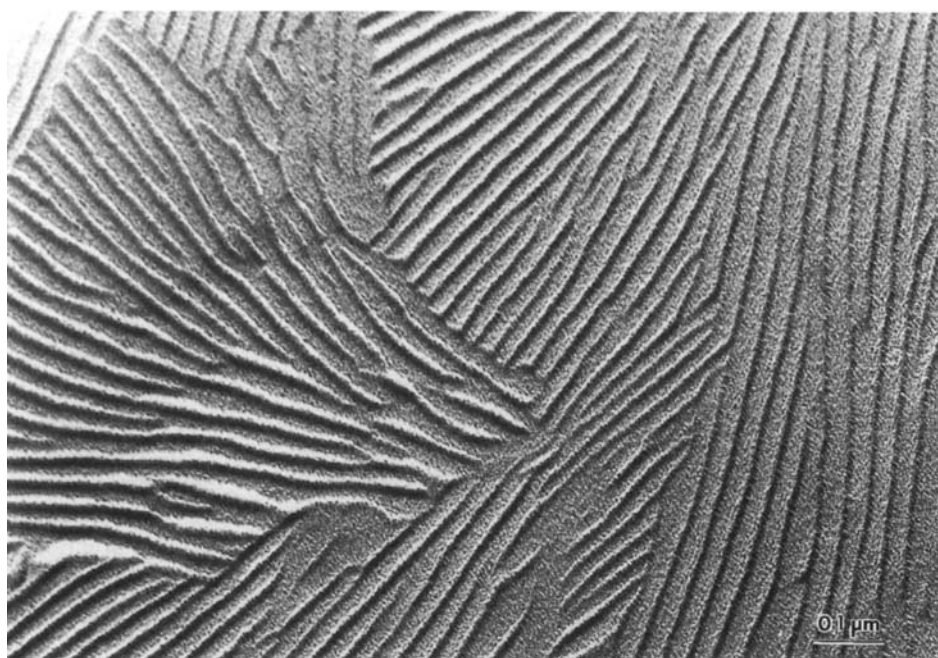


Figure 9. Transmission electron micrograph from the thinnest portion of a polymeric film in the  $\text{CrH}_c^*$  phase.

corresponding to the diffraction from reciprocal planes perpendicular to the side-chain axes. In tilted layers one expects the loss of intermolecular correlations as a result of displacements that occur only parallel to the side-chain axis direction. Therefore broad peaks are expected from reciprocal planes perpendicular to the side-chain axis. The  $d$ -spacings of the broader peaks indicate that the period in the side-chain axis direction is  $62.6 \text{ \AA}$ . Since the layer thickness is  $51.4 \text{ \AA}$ , the side-

chain axes must be tilted by  $34.8^\circ$  with respect to the layer normal.

According to the electron diffraction and X-ray diffraction results it is found that the unit cell of the polymer film has monoclinic symmetry and unit cell parameters are as follows;  $a = 10.06 \text{ \AA}$ ,  $b = 5.35 \text{ \AA}$ ,  $c = 62.6 \text{ \AA}$  and  $\beta = 124.8^\circ$ .

Figure 15 is a schematic representation of the bilayer structure of the  $\text{CrH}_c^*$  phase.



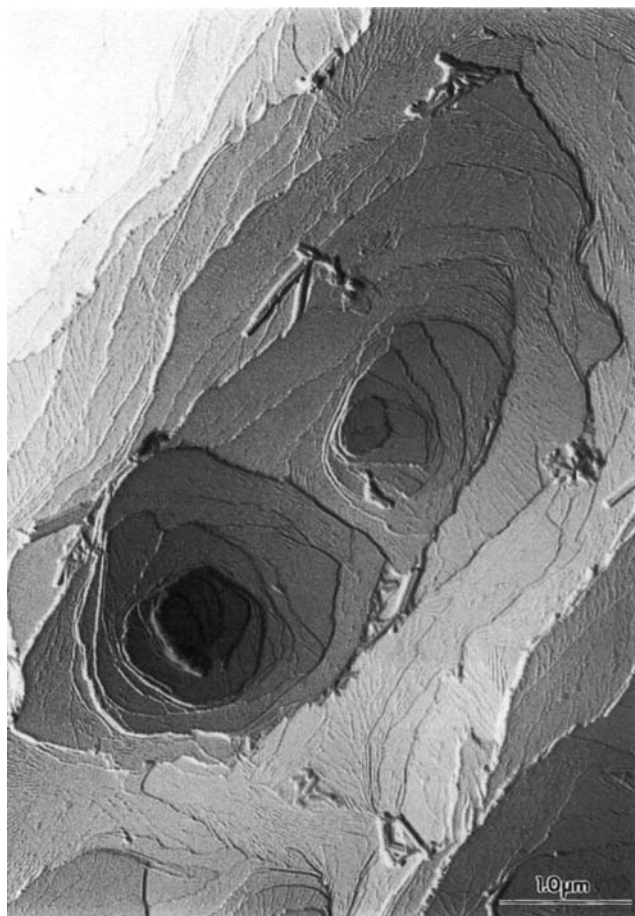


Figure 10. Transmission electron micrograph of a film of the side chain polymer prepared at the intermediate temperature of 95°C, showing morphologies characteristic of the CrE\* and the CrH<sub>c</sub>\* phases.

Usually in a chiral phase molecules are tilted with respect to the smectic layer normal and the molecular tilt directions twist in helical fashion as layers are traversed. This is the case of the S<sub>C</sub>\*<sup>+</sup>, S<sub>F</sub>\*<sup>+</sup>, S<sub>G</sub>\*<sup>+</sup>, S<sub>I</sub>\*<sup>+</sup> and S<sub>J</sub>\*<sup>+</sup> phases [13]. Gray and Goodby pointed out that ordered structures make the formation of this helical arrangement difficult. Hence it was their view that the CrH phase, with its almost crystalline structure, would not be likely to form a chiral phase [13]. It is therefore surprising to have observed here chiral modifications for the CrE phase (with side-chains parallel to the layer normal) and the tilted CrE phase (with its almost crystalline structure). In our case the *c* axis (the side-chain axis) direction is fixed for both CrE\* and CrH<sub>c</sub>\* and is perpendicular to the polymer film plane. The rotations of ±60° and 5.9° of the orthorhombic (CrE\*) and monoclinic (CrH<sub>c</sub>\*) lattices are about the *c* axis. The 5.9° twisting of lattices about the *c* axis between adjacent sublayers will not destroy the three-dimensional order because this angle is determined by the reciprocal lattice

parameters. The lattices in adjacent sublayers can therefore match each other. This has already been proved by the fact that the angle between every two neighbouring [110]\* or every two neighbouring [200]\* in the electron diffraction patterns is 5.9°. In the CrE\* phase reported here the *ab* lattice planes are rotated about the *c* axis from layer to layer and in the CrH<sub>c</sub>\* phase characterized here the *c*\* directions (the layer normal directions) change as layers are traversed. This is in contrast to other well-known chiral phases in which the *c*\* direction remains constant while moving from layer to layer. With regard to the observed ±60° rotations of *ab* lattice planes about the *c* axis in both CrE\* and CrH<sub>c</sub>\* sublayers, our current view is that such rotations probably involve dynamic phenomena.

We mentioned previously that the CrE\* phase is observed when the polymer solution is cast on glycerin heated to a temperature that is 33° higher than the temperature used in glycerin substrates which give rise to CrH<sub>c</sub>\* films. Our group reported previously [1, 2] that chiral CN groups in the molecules studied here react with each other at temperatures above 100°C to form imine bonds. In fact this reaction is a key step in the direction conversion of a monomer such as **S-1** or **R-1** to a two-dimensional polymer architecture. We therefore infer that the CrE\* phase observed in films cast on a hot substrate contains reacted nitriles, and thus its macromolecular architecture could be ladder-like or nearly two-dimensional in some regions of the film. On the other hand, films cast on a relatively colder substrate should experience less reaction, if any, among nitrile groups and thus have mostly the linear architecture of a comb polymer. In our view, the destruction of the tilt in the CrE\* phase is the consequence of at least partial reaction among stereocentres. In the structure of the 2D polymer system reported previously using **R-1** as the precursor, ±60° and 5.9° rotations disappear and the structure is a single crystal assembly. We believe this is the consequence of the two dimensional nature of the polymer architecture in which a higher degree of acrylate and nitrile reaction has taken place.

### 3.3. Phase transitions

We performed hot stage electron diffraction experiments in order to investigate the phase transitions of a thin film in the CrE\* phase. The objective of these experiments was to follow the evolution of molecular motions in this solid film as temperature was increased. Interestingly, the electron diffraction pattern of a free standing film changed dramatically at 67°C. Figure 16 shows the electron diffraction pattern obtained at this elevated temperature. This pattern no longer shows separated 110 and 200 reflections observed at room temperature and also the 5.9° rotation between adjacent

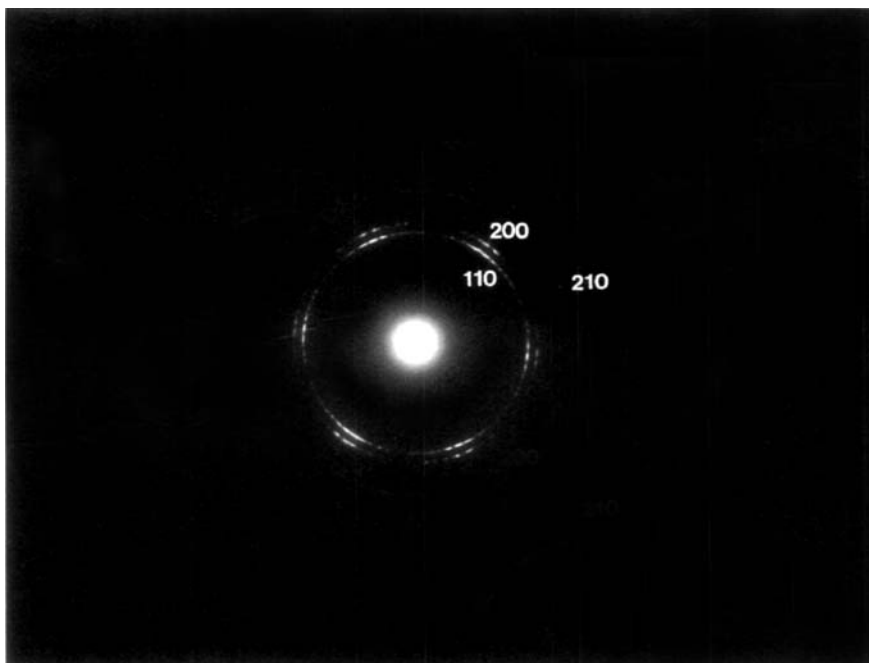


Figure 11. Selected area electron diffraction pattern from a domain of the  $\text{CrH}_c^*$  phase.

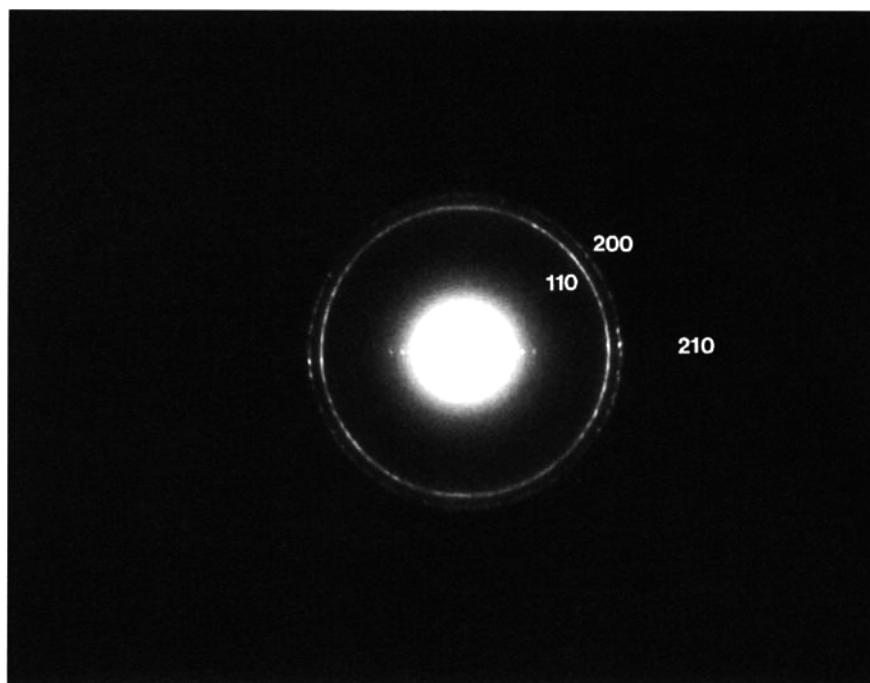


Figure 12. Selected area electron diffraction pattern of a thin film in the  $\text{CrH}_c^*$  phase tilted with respect to the beam direction.

sublayers in the  $\text{CrE}^*$  phase vanishes at  $67^\circ\text{C}$ . Instead, six strong reflections appear which are spaced at equal angles around the central spot and the whole pattern shows a reciprocal lattice plane with hexagonal geometry. This phase happens to be similar to that observed in the liquid crystal main chain copolymer *p*-hydroxybenzoate/*m*-hydroxybenzoate (95/5) at  $350^\circ\text{C}$

[14, 15]. Even though the distribution of electron diffraction spots in the pattern (see figure 16) has hexagonal geometry, the six innermost spots cannot be indexed with hexagonal unit cell parameters as  $100$ ,  $010$ ,  $\bar{1}10$ ,  $\bar{1}00$ ,  $0\bar{1}0$  and  $1\bar{1}0$  reflections in order to index the whole pattern. Therefore, the crystalline structure of the film does not have hexagonal symmetry, but still

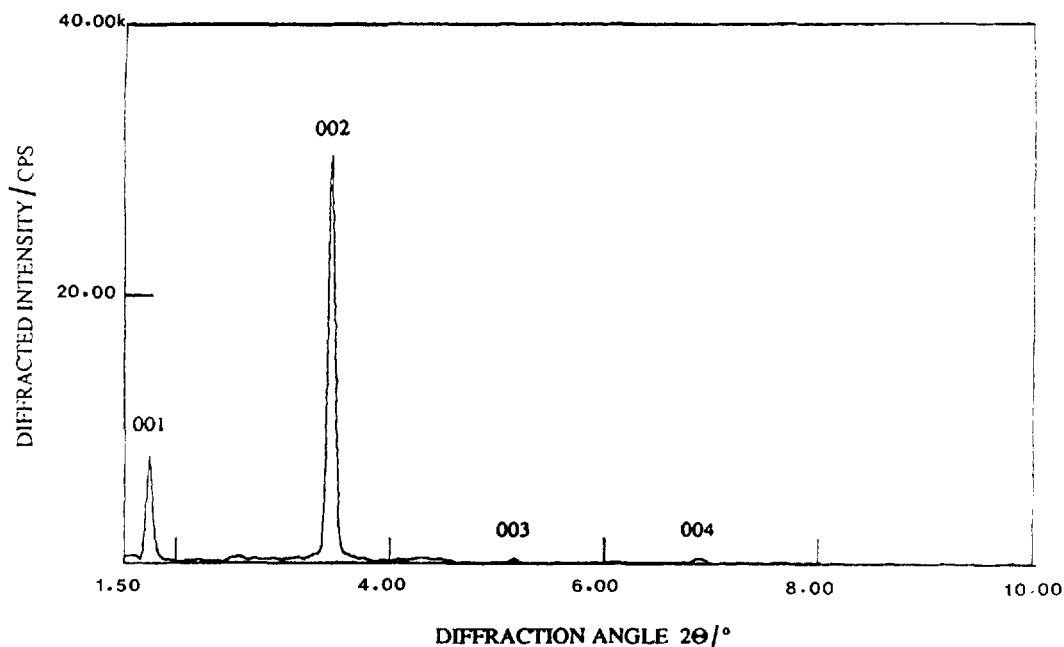


Figure 13. X-ray diffraction scan of a polymeric film in the  $\text{CrH}_c^*$  phase.

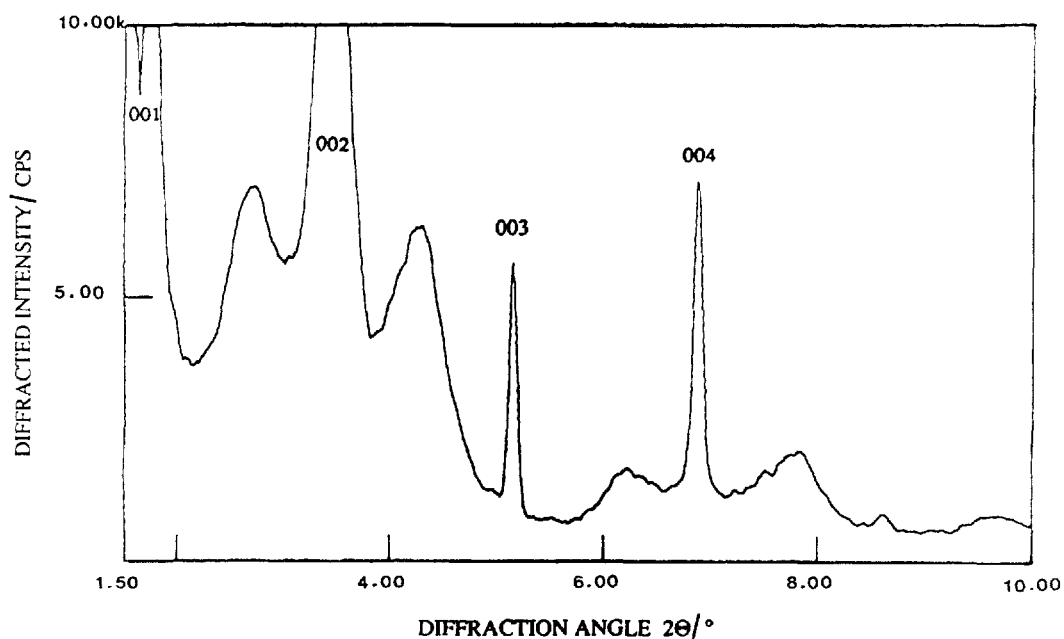


Figure 14. The X-ray diffraction scan shown in figure 13 with an enlarged intensity scale.

possesses orthorhombic symmetry. At the same time, this new phase is no longer a twisted chiral phase. The electron diffraction pattern can be interpreted in terms of three different orientations of orthorhombic reciprocal lattices with  $b^* = 3^{1/2}a^*$  related to one another by rotations of  $\pm 60^\circ$  about the  $c$  axis (see figure 17). From figure 17 it is clear that this interpretation results in an array of diffraction spots with hexagonal geometry (see

figure 18). Since the distribution of electron diffraction spots in figure 16 is in a hexagonal geometry, the electron diffraction pattern can be first indexed according to the hexagonal reciprocal lattice plane shown in figure 18. Then, the corresponding indices of orthorhombic lattices can be easily found comparing figures 18 and 17. The observed  $d$ -spacings and their indices are listed in table 3, and the following orthorhombic unit cell parameters

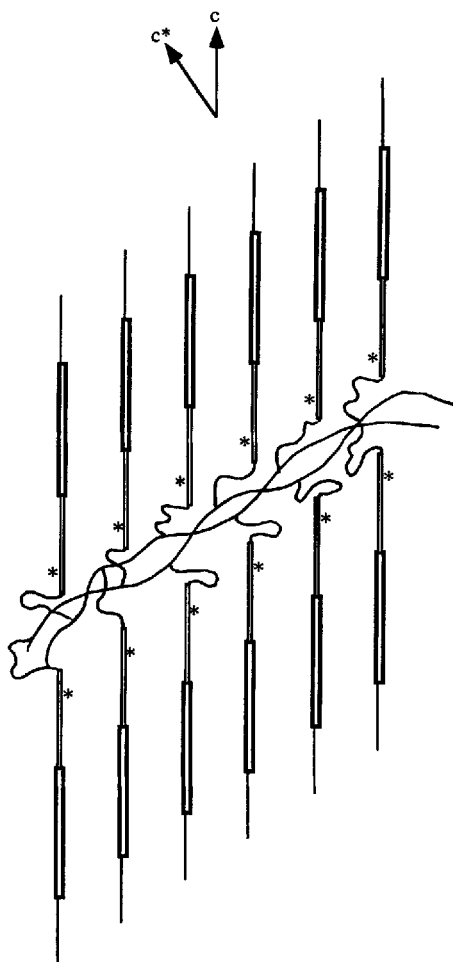


Figure 15. Schematic representation of a tilted bilayer of the  $\text{CrH}_c^*$  phase, showing side-chains packed in parallel with polymer backbones and spacers confined in a thin disordered region between two mesogenic sublayers.

can be determined from the data;  $a=8.80 \text{ \AA}$ ,  $b=5.08 \text{ \AA}$  and  $\gamma=90^\circ$ .

It is obvious that there is long range positional order as well as bond orientational order in the film at  $67^\circ\text{C}$ . The structure of the polymer at  $67^\circ\text{C}$  may therefore be described as a crystal smectic  $\text{E}_h$  phase ( $\text{CrE}_h$ ) with the subscript h denoting the hexagonal geometry of the

Table 1. Crystallographic data for the polymeric  $\text{CrE}^*$  phase.

Interplanar spacing $d/\text{\AA}$	Miller indices, $hk0$	Interplanar spacing $d/\text{\AA}$	Miller indices, $hk0$
4.48	110	2.44	310
4.12	200	2.24	220
3.26	210	1.91	320
2.54	120	1.91	410

Table 2. Crystallographic data for the polymeric  $\text{CrH}_c^*$  phase.

Interplanar spacing $d/\text{\AA}$	Miller indices, $hk0$
4.49	110
4.13	200
3.26	210

pattern as a result of  $b^*$  being equal to  $3^{1/2}a^*$ . It is not clear to us what is the nature of the change in local interactions or molecular conformation which leads to the observed expansion of the  $a$  axis and contraction of the  $b$  axis resulting in  $a = 3^{1/2}b$ . It is interesting that a similar phase was observed in a structurally similar main chain aromatic polyester studied in our laboratory [3] and also in an aromatic ester copolymer with a completely different structure [14, 15]. Therefore, there is some phenomenon that is generic about the nature of the local structure in these aromatic esters. This phenomenon could be related to conformational changes or the relative importance of dispersive versus dipolar forces at different temperatures. The structure of the  $\text{CrE}_h$  phase is different from that of crystal E phase ( $\text{CrE}$ ) in which  $b^* \neq 3^{1/2}a^*$ .

When the thin film is heated to  $91^\circ\text{C}$ , reflections such as the 210, 120, and others disappear from the diffraction pattern. At this temperature only six reflections remain in the pattern which are distributed with hexagonal geometry but in contrast to spots in the patterns of the  $\text{CrE}_h$  phase, these reflections can be indexed by hexagonal unit cell parameters as 100, 010,  $\bar{1}10$ ,  $\bar{1}00$ ,  $0\bar{1}0$  and  $1\bar{1}0$  (see figure 19). We therefore have hexagonal symmetry at  $91^\circ\text{C}$  and at this temperature the intermolecular distance has increased as indicated by the  $d$ -spacings. At  $67^\circ\text{C}$   $d_{200} = 4.40 \text{ \AA}$  whereas at  $91^\circ\text{C}$  the corresponding  $d$ -

Table 3. Crystallographic data for the polymeric  $\text{CrE}_h$  phase.

Interplanar spacing $d/\text{\AA}$	Miller indices, $hk0$	
	Hexagonal lattice	Orthorhombic lattice
4.40	200,020, $\bar{2}20$ , $\bar{2}00$ ,0 $\bar{2}0$ , $\bar{2}20$	200,110, $\bar{1}10$ , $\bar{2}00$ , $\bar{1}\bar{1}0$ , $1\bar{1}0$
3.33	210,120,130, $\bar{2}30$ , $\bar{3}20$ , $\bar{3}10$ $\bar{2}\bar{1}0$ , $\bar{1}\bar{2}0$ , $\bar{1}30$ , $\bar{2}\bar{3}0$ , $\bar{3}\bar{2}0$ , $\bar{3}\bar{1}0$	210, $\bar{2}\bar{1}0$ , $\bar{2}10$ , $\bar{2}\bar{1}0$
2.54	220,240, $\bar{4}20$ , $\bar{2}20$ , $\bar{2}40$ , $\bar{4}20$	020,0 $\bar{2}0$ ,310, $\bar{3}\bar{1}0$ , $\bar{3}10$ , $\bar{3}\bar{1}0$
2.20	400,040, $\bar{4}40$ , $\bar{4}00$ ,040, $\bar{4}40$	400, $\bar{4}00$ , $\bar{2}20$ , $\bar{2}20$ , $\bar{2}20$ , $\bar{2}20$

Figure 16. Electron diffraction pattern obtained at 67°C of a film that was in the CrE\* phase at room temperature. At this elevated temperature a transition has occurred into the CrE<sub>h</sub> phase (see text). Reflections in the pattern are indexed according to the reciprocal lattice plane shown in figure 18.

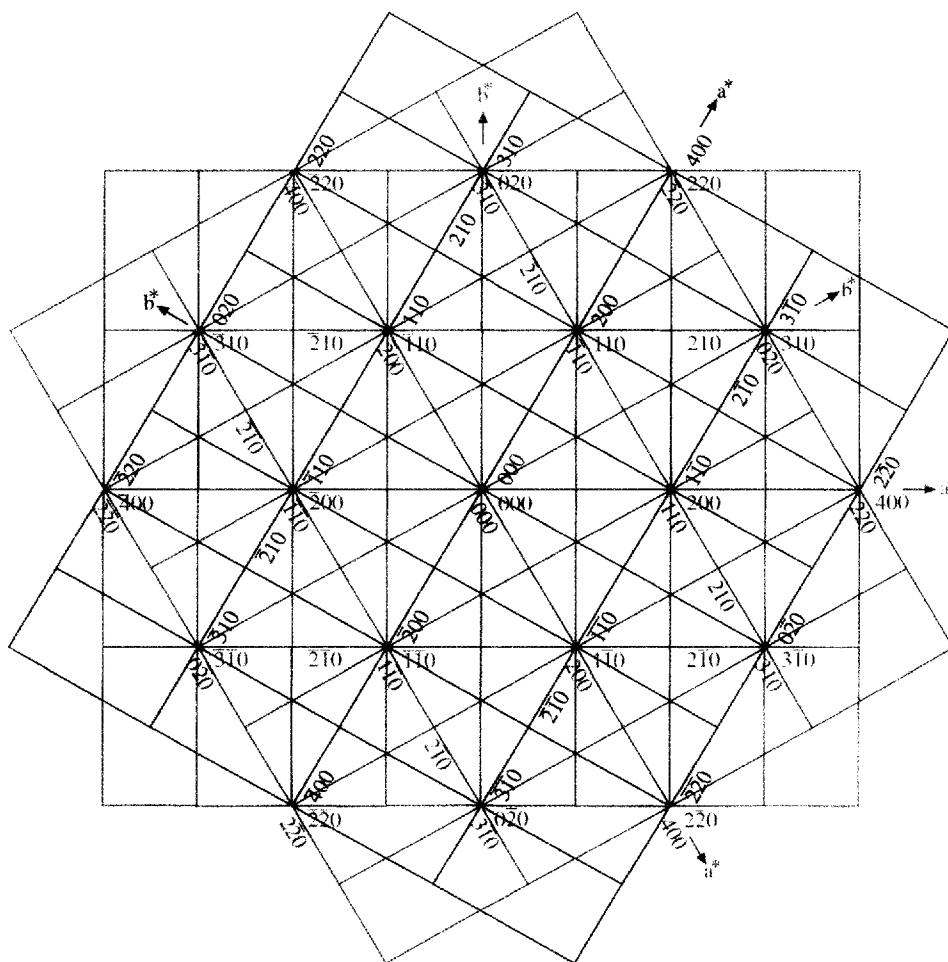
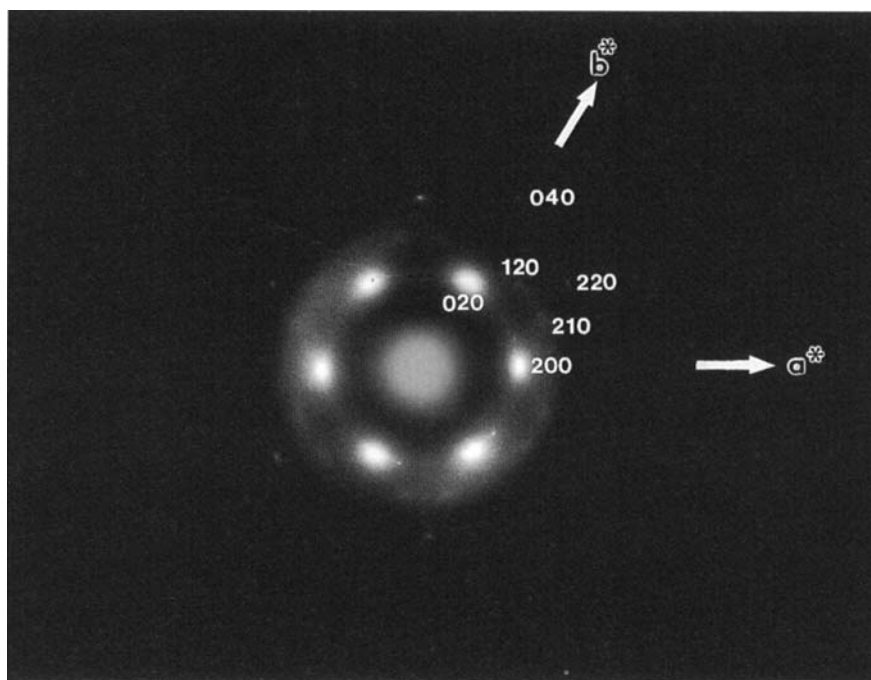


Figure 17. Schematic representation of three identical orthorhombic  $a^*b^*$  reciprocal lattice planes with  $b^* = 3^{1/2}a^*$  related to one another by rotations of  $\pm 60^\circ$  about the  $c$  axis.

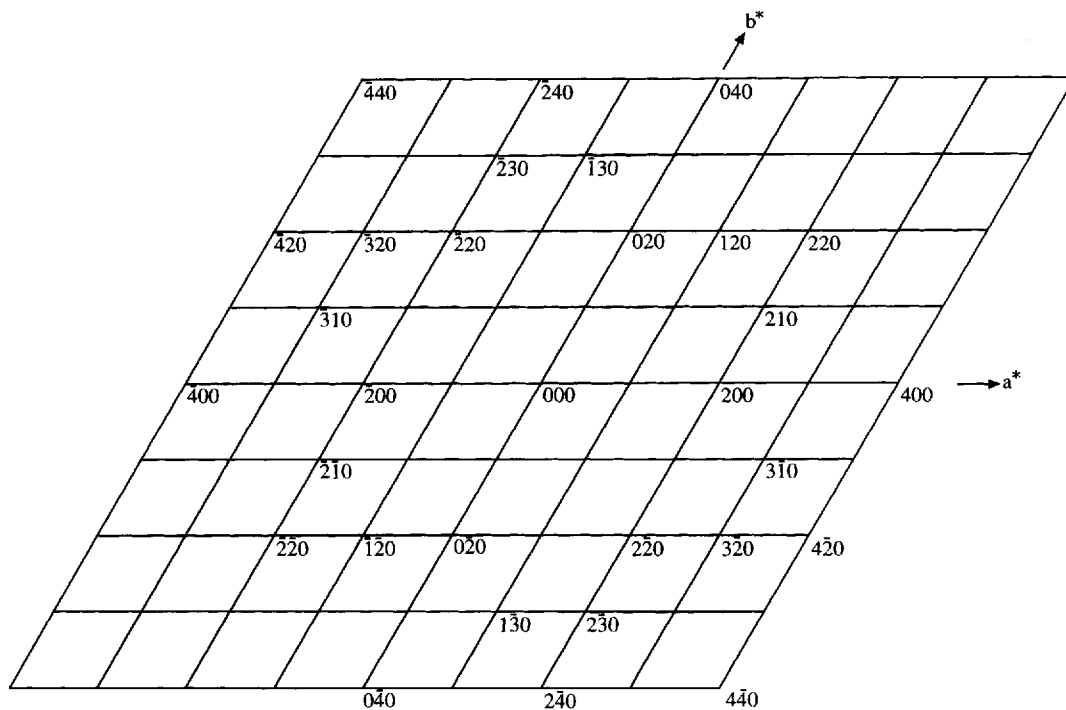


Figure 18. Schematic representation of the  $a^*b^*$  reciprocal lattice planes in figure 17, resulting from three identical orthorhombic reciprocal lattice planes with  $b^* = 3^{1/2}a^*$  related to one another by rotations of  $\pm 60^\circ$  about the  $c$  axis. The resulting reciprocal lattice plane exhibits a hexagonal geometry.

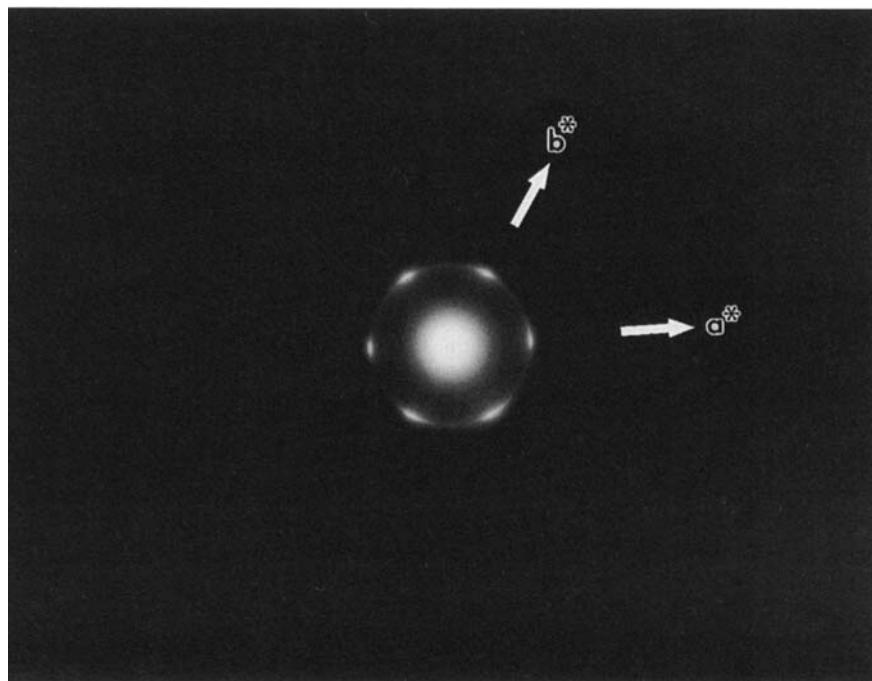


Figure 19. Electron diffraction pattern obtained at  $91^\circ\text{C}$  of the film in the  $\text{CrE}^*$  phase at room temperature, revealing a hexatic smectic B phase at this elevated temperature.

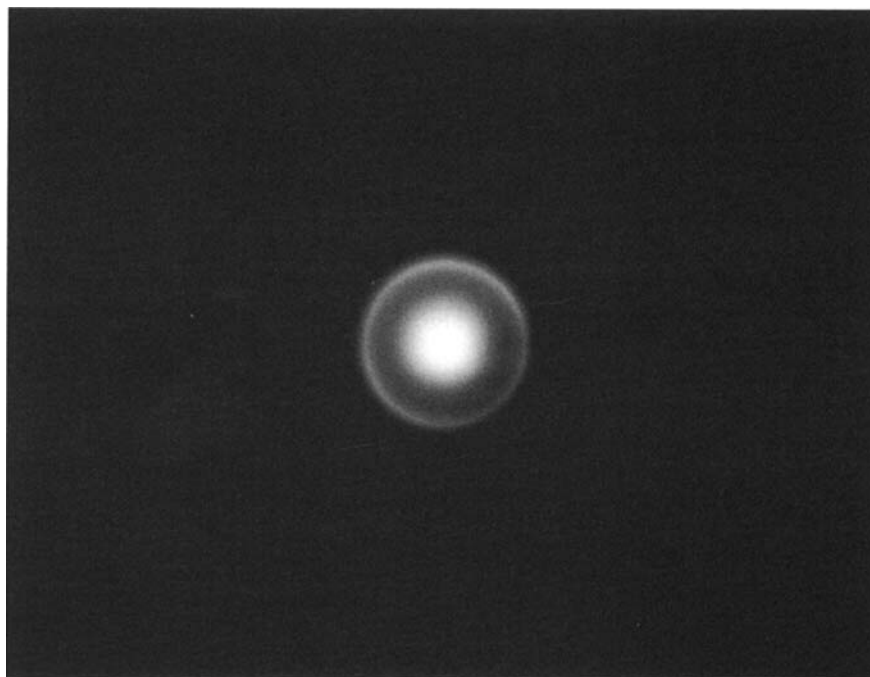
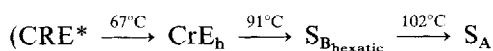


Figure 20. Electron diffraction pattern obtained at 102°C of the film in the CrE\* phase at room temperature, revealing the existence of a smectic A phase at this temperature.

spacing is equal to 4.43 Å. The small increase in intermolecular distance probably leads to independent rotation of the side chains, changing the nature of positional order of side chains from long range to short range. However, long range hexagonal bond orientational order still remains and the phase at 91°C is therefore a hexatic smectic B phase [13, 16, 17]. Finally, when samples are heated to 102°C the bond orientational order is short range as revealed by the diffuse ring in the electron diffraction pattern shown in figure 20. At 102°C the film has the structure characteristic of a smectic A phase in which the layered arrangement is preserved. All phase transitions observed are reversible upon cooling and are thus described by the following phase sequence:

Chiral crystal E phase  $\rightleftharpoons$  Crystal smectic E<sub>h</sub> phase  
 $\rightleftharpoons$  Hexatic smectic B phase  $\rightleftharpoons$  smectic A phase



#### 4. Conclusions

Two novel smectic bilayer structures have been identified in an enantiomerically enriched chiral side chain polymer containing the highly dipolar nitrile group at stereocentres. One of the structures which we denote as CrE\* has the unusual feature of having its side chains arranged parallel to the layer normal in spite of its enantiomeric bias and twisted nature. In the second structure denoted as CrH<sub>c</sub>\* side chains are tilted with

respect to the layer normal but the layers are regularly twisted about the side-chain axis (*c* axis) and not about the layer normal (*c*\* axis) as it is commonly found in chiral phases. Interestingly, in both of these bilayer structures each sublayer contains three different orientations of orthorhombic or monoclinic lattices which are related to one another by rotations of  $\pm 60^\circ$  about the *c* axis (side-chain axis). The phase transition sequence followed by the CrE\* phase appears to be common in various polymeric materials based on aromatic esters.

This work was supported through grant DE AC02 76ER01198 from the Department of Energy and obtained through the Materials Research Laboratory at the University of Illinois.

#### References

- [1] STUPP, S. I., SON, S., LIN, H. C., and LI, L. S., 1993, *Science*, **259**, 59.
- [2] STUPP, S. I., SON, S., LI, L. S., LIN, H. C., and KESER, M., 1995, *J. Am. chem. Soc.*, **117**, 5212.
- [3] LI, L. S., and STUPP, S. I., 1995, *Macromolecules*, **28**, 2618.
- [4] MOORE, J. S., and STUPP, S. I., 1992, *J. Am. chem. Soc.*, **114**, 9.
- [5] MOORE, J. S., and STUPP, S. I., 1990, *J. Org. Chem.*, **55**, 3374.
- [6] DAVIDSON, P., and LEVELUT, A. M., 1992, *Liq. Cryst.*, **11**, 469.
- [7] GOODBY, J. W., NISHIYAMA, I., SLANEY, A. J., BOOTH, C. J., and TOYNE, K. J., 1993, *Liq. Cryst.*, **14**, 37.

- [8] DE GENNES, P. G., 1972, *Sol. St. Commun.*, **10**, 753.
- [9] RENN, S. R., and LUBENSKY, T. C., 1988, *Phys. Rev. A.*, **38**, 2132.
- [10] GOODBY, J. W., WAUGH, M. A., STEIN, S. M., CHIN, E., PINDAK, R., and PATEL, J. S., 1989, *J. Am. chem. Soc.*, **111**, 8119.
- [11] SRAJER, G., PINDAK, R., WAUGH, M. A., GOODBY, J. W., and PATEL, J. S., 1990, *Phys. Rev. Lett.*, **64**, 1545.
- [12] IHN, K. J., ZASADZINSKI, J. A. N., PINDAK, R., SLANEY, A. J., and GOODBY, J. W., 1992, *Science*, **258**, 275.
- [13] GRAY, G. W., and GOODBY, J. W., 1984, *Smectic Liquid Crystals-Textures and Structures*.
- [14] LI, L. S., LIESER, G., ROSENAU-EICHIN, R., and FISCHER, E. W., 1987, *Makromol. Chem., Rap. Commun.*, **8**, 159.
- [15] LI, L. S., 1989, *Makromol. Chem., Rap. Commun.*, **10**, 307.
- [16] BROCK, J. D., BIRGENEAU, R. J., LITSTER, J. D., and AHARONG, A., 1989, *Phys. Today*, 52.
- [17] PERSHAN, P. S., 1988, *Structure of Liquid Crystal Phases* (World Scientific, Singapore) Chap. 1.